Regular Biorthogonal Linear-Phase Filter Banks: Theory, Structure and Application in Image Coding

Soontorn Oraintara*[1], Trac Tran[2], Truong Nguyen[3]
[1]University of Texas at Arlington, EE Dept., Arlington, TX
oraintar@uta.edu
[2]The Johns Hopkins University, ECE Dept., Baltimore MD
trac@jhu.edu
[3]University of California San Diego, ECE Dept., San Diego, CA
nguyent@ece.ucsd.edu

Abstract— **This paper discusses a method of regularity imposition onto biorthogonal linear-phase M-band filter banks using the lattice structure. A lifting structure is proposed for lattice matrix parameterization where regularity constraints can be imposed. The paper focuses on cases with analysis and synthesis filter banks having up to two degrees of regularity. In each case, at least one design example is presented. Simulation results from an image coding application also shows that these transforms perceptually outperform the conventional regular paraunitary linear-phase filter banks.**

SP EDICS: 2-SPTM Filter Bank Design and Theory

*Contact author: Professor Soontorn Oraintara
E-mail: oraintar@uta.edu
University of Texas at Arlington
Department of Electrical Engineering
Box 19016, 416 Yates St.
Arlington, TX 76019-0016, USA
Tel: (817) 272-3482, Fax: (817) 272-2253

I. Introduction

Wavelets and filter banks have established themselves as powerful tools in transform-based signal compression applications [1]. They are used to remove spatial signal redundancy in many video, image and audio coding standards such as MPEG video, JPEG, MPEG audio [2]. Figure 1 shows the general block diagram of a transform-based signal coding algorithm. The input signal is represented as a linear combination of the transform basis functions and their corresponding coefficients, the so called transform coefficients, are obtained at the output of the transform block. These coefficients are then efficiently quantized and entropy coded to the coder output. In this paper, we focus on still image coding as an application of transform-based signal compression while other applications can also be naturally applied.

There has been considerably interest in designing the transform that yields high perceptual reconstructed quality while keeping the computational cost low. At the earlier stage, the discrete cosine transform (DCT) was first employed as an efficient transform for the JPEG image coding standard where the bases are truncated cosine functions, having equal length, linear phase, orthogonality and uniform localization in frequency domain. However, at low bit rates, the reconstruction usually suffers from blocking artifact due to the discontinuity at the borders of the basis functions. The discrete wavelet transform is a more recent technique employed in transform-based image coder in order to reduce or eliminate blocking artifacts. Constructed by iterating on the lowpass branch of a two-channel perfect reconstruction (PR) filter bank, the entire frequency domain is octavely divided, rendering a multiscale image representation. Perhaps the most popular wavelet filter pair used in practical image coders is the (9/7)-tap linear phase biorthogonal wavelet which has also been used in the FBI's fingerprint compression standard [3] and now in JPEG2000 [4]. Combining the advantages of efficient implementation of the DCT and the overlapping basis functions of wavelets, lapped transforms (LT) have been recently studied and found to often outperform the previous two conventional techniques [5], [6], [7].

The transforms for image coding can be categorized into two major classes: block-based and wavelet-based. Block transforms can be constructed by uniform M-channel filter banks such as DCT [8], LOT [5], GenLOT [6], and wavelet transforms can be generated by iterating two-channel filter banks on the lowpass channel [1]. In transforms of both families, all filter impulse responses have real values with linear-phase (LP) responses (symmetric or antisymmetric). The linearity of the phase responses is to eliminate the phase distortion and to allow symmetric extension at the border of the image.

Figure 2(a) shows a uniform maximally decimated M-channel filter bank which consists of the analysis filters $H_i(z)$ and synthesis filters $F_i(z)$. The M-fold downsampling at the analysis side indicates that the total sampling rate at the input of the processing block is equal to that of the original input signal. Figure 2(b) illustrates the equivalent polyphase structure where $\mathbf{E}(z)$ and $\mathbf{R}(z)$ are the type-I and type-II polyphase matrices of the analysis filters $H_i(z)$ and synthesis filters $F_i(z)$ respectively [9]. It is obvious that the filter bank is PR if $\mathbf{E}(z)$ and $\mathbf{R}(z)$ are inverse of each other.

A fundamental concept in wavelet theory is regularity.

The degree of regularity is closely related to the smoothness of the basis functions – a critical component in smooth reconstruction. The degree of regularity is also equivalent to the vanishing moments in the bandpass filters [10], [11], [12]. In both paraunitary (PU) and biorthogonal (BO) cases, the regularity of a transform is defined as the number of multiple zeros at the mirror frequencies:

Definition 1: An M-band filter bank is said to be (K_a, K_s)-regular if the analysis and synthesis lowpass filters $H_0(z)$ and $F_0(z)$ have, respectively, at least K_a and K_s zeros at $\frac{2\pi k}{M}$ for $k = 1, \cdots, M-1$.

In the PU case, the degrees of regularity of the analysis and synthesis filter banks are equal since their impulse responses are time-reversed, and hence the regularity degree of the filter bank can be identified by using one number instead of an order pair. In the BO case, the analysis and synthesis lowpass filters can be different and thus their degrees of regularity may not be the same. For a K-regular PU filter bank, the bandpass filters of the analysis and synthesis filters have K vanishing moments, i.e. $\sum_n n^\ell h_i(n) = 0$ for $\ell = 0,\ 1,\ \cdots,\ K-1$. For a (K_a, K_s) BO filter bank, the analysis and synthesis bandpass filters, respectively, have K_s and K_a vanishing moments.

In image coding application, the analysis filters should be optimized to obtain maximum coding gain, i.e. the magnitude response must match the signal spectrum with high stopband attenuation for maximum decorrelation [13]. On the other hand, the synthesis filters should be optimized to yield smooth basis functions. This can be accomplished by imposing a number of zeros at mirror frequencies into the synthesis lowpass filter. Therefore, the cost functions for the optimization of $H_i(z)$ and $F_i(z)$ should be different. In the PU case, since $f_i(n)$ are simply the time-reversed versions of $h_i(n)$, they can not be optimized for different purposes. In the BO case, the frequency responses of $H_0(z)$ and $F_0(z)$ can be different and they can have different numbers of zeros at mirror frequencies. In practice, $F_0(z)$ should have more zeros in order to obtain smooth synthesis basis functions. At the same time, the analysis bandpass and highpass filters should have a high number of vanishing moments in order to obtain superior energy compaction at low frequency band. This paper presents a method to impose one and two degrees of regularity into $H_0(z)$ and $F_0(z)$ using lattice structures of BOLP filter banks.

A. Organization

In this paper, we introduce a novel approach of imposing up to two vanishing moments directly onto the lattice structure of M-channel BOLP filter banks. Section II reviews the lattice structure of BOLP filter banks. Their relations to the transform's regularity are presented in section III. In section IV, a method for imposing these conditions onto the lattice components is discussed with numerous design examples. Image coding examples are presented in section V, and section VI concludes the paper.

B. Notations

Bold-faced lower case characters are used to denote vectors while bold-faced upper case characters are used to denote matrices. $\mathbf{A}^T$, $\mathbf{A}^{-1}$ and $|\mathbf{A}|$ denote respectively the transpose, the inverse and the determinant of the matrix $\mathbf{A}$. The symbols $h_i[n]$, $H_i(z)$, and $H_i(e^{j\omega})$ stand for the i-th filter's impulse response, its associated z-transform, and its Fourier transform.

Several special matrices with reserved symbols are: the polyphase matrix of the analysis bank $\mathbf{E}(z)$, the polyphase matrix of the synthesis bank $\mathbf{R}(z)$, the identity matrix $\mathbf{I}$, the reversal matrix $\mathbf{J}$, the null matrix $\mathbf{0}$, a permutation matrix $\mathbf{P}$, and the diagonal matrix with entries being either $+1$ or -1 $\mathbf{D}$. Likewise, the special vectors are: the column vector with all entries being unity $\mathbf{1}$ and the column vector with all entries being zero except the first entry being unity $\mathbf{a}$. When the size of a matrix or vector is not clear from context, subscripts will be included. M and K are usually reserved for the number of channels and the degrees of regularity. An M-channel MN-tap FB is sometimes denoted as an $M \times MN$ lapped transform where N is the overlapping factor. For abbreviations, we often use LP, PR, PU, and FB to denote *linear phase*, *perfect reconstruction*, *paraunitary*, and *filter bank*.

II. A Lattice Structure for BOLP Filter Banks

The lattice structure is an efficient implementation of filter banks or lapped transforms with linear-phase basis functions [6], [7]. In this paper, it is assumed that the number of channels $M \geq 4$ is even, and all the filters have equal length NM where N is an integer. It has been proven that when the number of channels is even, there are $\frac{M}{2}$ symmetric and $\frac{M}{2}$ anti-symmetric filters [14]. The polyphase matrix $\mathbf{E}(z)$ is an $M \times M$ polynomial matrix in z of order $(N-1)$. Under the assumptions on M, N and the filter symmetry, the lattice elements can be defined as follows:

$$\mathbf{\Gamma}_i = \begin{bmatrix} \mathbf{U}_i & \mathbf{0}_L \\ \mathbf{0}_L & \mathbf{V}_i \end{bmatrix}, \quad \mathbf{W} = \frac{1}{\sqrt{2}} \begin{bmatrix} \mathbf{I}_L & \mathbf{I}_L \\ \mathbf{I}_L & -\mathbf{I}_L \end{bmatrix},$$

$$\mathbf{\Lambda}(z) = \begin{bmatrix} \mathbf{I}_L & \mathbf{0}_L \\ \mathbf{0}_L & z^{-1}\mathbf{I}_L \end{bmatrix}, \quad \text{and} \quad \widetilde{\mathbf{I}} = \begin{bmatrix} \mathbf{I}_L & \mathbf{0}_L \\ \mathbf{0}_L & \mathbf{J}_L \end{bmatrix}$$

where $L = \frac{M}{2}$ and $\mathbf{J}$ is the reversal matrix. $\mathbf{U}_i$ and $\mathbf{V}_i$ are nonsingular matrices of size $L \times L$. For PU filter banks, these matrices are orthonormal and each of them can be parameterized using $\binom{L}{2}$ rotation angles [9]. For BO filter banks, these $\mathbf{U}_i$ and $\mathbf{V}_i$ matrices are nonsingular and there are L^2 free parameters in each matrix. The polyphase matrix $\mathbf{E}(z)$ of a LP filter bank with degree $N-1$ can be factored as a product of nonsingular polynomial matrices with degree one [6], [7], i.e.,

$$\mathbf{E}(z) = \mathbf{G}_{N-1}(z)\mathbf{G}_{N-2}(z)\cdots\mathbf{G}_1(z)\mathbf{E}_0 \qquad (1)$$

where $\mathbf{G}_i(z) = \mathbf{\Gamma}_i\mathbf{W}\mathbf{\Lambda}(z)\mathbf{W}$ and $\mathbf{E}_0 = \mathbf{\Gamma}_0\widetilde{\mathbf{I}}\mathbf{W}$. Hence a causal synthesis polyphase matrix $\mathbf{R}(z)$ can be given by:

$$\mathbf{R}(z) = z^{1-N}\mathbf{E}_0^{-1}\mathbf{G}_1^{-1}(z)\cdots\mathbf{G}_{N-2}^{-1}(z)\mathbf{G}_{N-1}^{-1}(z) \qquad (2)$$

Figure 3 shows the lattice structure of BOLP filter banks. Although this structure is minimal the terms of the number of delays, it does not minimize the number of free parameters. In [15], [12], the authors show that the matrices $\mathbf{U}_i$ for $i>0$ can be set to $\mathbf{I}$ without any completeness violation. This more efficient structure with

$$\mathbf{U}_i \equiv \mathbf{I} \text{ for } i>0$$

will be used throughout the analysis of this paper.

III. Relationship Between the Lattice Structure and Filter Bank's Regularity

The theory of regular M-band wavelets and filter banks has been well established. Here we only summarize their important properties. Let us denote $\phi(t)$ and $\psi_i(t)$ ($i=1,2,\ldots,M-1$) as the synthesis scaling function and wavelets, and let $\widetilde{\phi}(t)$ and $\widetilde{\psi}_i(t)$ ($i=1,2,\ldots,M-1$) be the analysis scaling function and wavelets. These functions satisfy the dilation and wavelet equations [1] as follows:

$$\begin{aligned}
\widetilde{\phi}(t) &= M\sum_k h_0(k)\widetilde{\phi}(Mt-k)\\
\phi(t) &= M\sum_k f_0(k)\phi(Mt-k)\\
\widetilde{\psi}_i(t) &= M\sum_k h_i(k)\widetilde{\phi}(Mt-k)\\
\psi_i(t) &= M\sum_k f_i(k)\phi(Mt-k).
\end{aligned}$$

Since the filter bank is PR, it is straight forward to show that

$$\begin{aligned}
\int \phi(t-k)\widetilde{\phi}(t-\ell) &= \delta(k-\ell),\\
\int \psi_i(t-k)\widetilde{\psi}_j(t-\ell) &= \delta(i-j)\delta(k-\ell),\\
\int \phi(t-k)\widetilde{\psi}_i(t-\ell) &= 0,\\
\int \widetilde{\phi}(t-k)\psi_j(t-\ell) &= 0.
\end{aligned}$$

From Definition 1, the regularity of filter banks was defined the analysis and synthesis lowpass filters in frequency domain. The conditions can also be expressed in other forms as summarized below:

Proposition 1: For a (K_a,K_s)-regular filter bank, the following statements are true:

1. The analysis (synthesis) bandpass and highpass filter $H_i(z)$ ($F_i(z)$), $i=1,2,\ldots,M-1$, have K_s (K_a) multiple zeros at the DC frequency ($z=1$).
2. Polynomial sequences up to degree K_s-1 (K_a-1) are rejected by the analysis (synthesis) bandpass and highpass filters, and are captured by the analysis (synthesis) lowpass filter. In other words,
 (a) $\sum_n n^k h_i(n)=0$, $i=1,2,\ldots,M-1$, for $0\le k\le K_s-1$, and
 (b) $\sum_n n^k f_i(n)=0$, $i=1,2,\ldots,M-1$, for $0\le k\le K_a-1$.
3. The first K_s (K_a) moments of $\psi_i(t)$ ($\widetilde{\psi}_i(t)$) are zero for all $i=1,2,...,M-1$.
4. If $g(t)$ has K_s derivatives then $\left|\int g(t)\widetilde{\psi}_i(M^jt-k)dt\right| = O(M^{-jK_s})$, where O suggests order of its argument [16].
5. $\left\|g(t)-\sum_k a_{jk}\phi(M^jt-k)\right\| = O(M^{-jK_s})$.
6. The downsampling matrix

$$\mathbf{L} = (\downarrow M)M\mathbf{H}_0 = M\begin{bmatrix} h_0(0) & \cdots & h_0(M) & \cdots\\ 0 & \cdots & h_0(0) & \cdots\\ \vdots & \vdots & \vdots & \vdots \end{bmatrix}$$

has eigenvalues $1,\ \frac{1}{M},\ \cdots,\ \left(\frac{1}{M}\right)^{K_s-1}$.

Conditions 1. and 2. express the regularity of the filter bank in terms of the vanishing moments of the bandpass filters in frequency domain and time domain, respectively. These conditions have been translated to the wavelet domain in condition 3. Conditions 4. and 5. relate the regularity to smoothness of these basis functions. Finally, they are expressed in the eigenvalue domain in condition 7. These conditions are useful and can be used to test the regularity of a filter bank in different situations. The proofs of Proposition 1 can be found in the Appendix.

Next, in order to impose the regularity into the lattice structure, equivalent relations in terms of the polyphase matrices need to be established.

Theorem 1: A filter bank is (K_a,K_s)-regular if and only if its polyphase matrices $\mathbf{E}(z)$ and $\mathbf{R}(z)$ satisfy the following conditions:

$$\frac{d^n}{dz^n}\left\{[1\ z^{-1}\ \cdots\ z^{1-M}]\mathbf{E}^T(z^M)\right\}\Big|_{z=1} = [c_n\ 0\ \cdots\ 0]. \quad (3)$$

$$\frac{d^m}{dz^m}\left\{[1\ z^{-1}\ \cdots\ z^{1-M}]\mathbf{R}(z^M)\right\}\Big|_{z=1} = [d_m\ 0\ \cdots\ 0]. \quad (4)$$

where $n=0,\cdots,K_s-1$; $m=0,\cdots,K_a-1$; and $\{c_n,d_m\}$ are some non-zero constants. [12], [17].

Equations (3) and (4) can be expressed in terms of the lattice elements $\mathbf{U}_0$ and $\mathbf{V}_i$. Since the calculation is straightforward but the expressions are very cumbersome, we shall present the results only for the cases of (K_a,K_s)-regular BOLP filter banks with $K_a,K_s\le 2$. Substituting $\mathbf{G}_i(z)$ and $\mathbf{E}_0$ into (3) and (4) for the cases of $n,m\le 1$ yields the following conditions (see next page):

where $\mathbf{b}_L = \frac{1}{2L}[1\ 3\ \cdots\ 2L-1]^T$. The proof of these conditions can be done directly by substituting the factorization of the polyphase matrices into (3) and (4). Similar derivation for orthogonal case can be found in the Appendix of [18] and thus the proof shall be omitted here.

In a (K_a,K_s)-regular filter bank, a combination of the above conditions must be satisfied as follows:

Filter bank	Necessary and sufficient conditions
(1,1)-regular	A_{01}, A_{10}
(1,2)-regular	A_{01}, A_{10}, A_{02}
(2,1)-regular	A_{01}, A_{10}, A_{20}
(2,2)-regular	A_{01}, A_{10}, A_{02}, A_{20}

$$\begin{array}{lrcl}
A_{01}(n=0): & \mathbf{U}_0\mathbf{1}_L & = & c_0\mathbf{a}_L \\
A_{10}(m=0): & \mathbf{U}_0^{-T}\mathbf{1}_L & = & d_0\mathbf{a}_L \\
A_{02}(n=1): & \sqrt{L}\mathbf{a}_L + \sqrt{L}\sum_{j=2}^{N-1}\prod_{i=N-2}^{N-j}\mathbf{V}_i\mathbf{a}_L + \prod_{i=N-2}^{0}\mathbf{V}_i\mathbf{b}_L & = & \mathbf{0}_L \\
A_{20}(m=1): & \sqrt{L}\mathbf{a}_L + \sqrt{L}\sum_{j=2}^{N-1}\prod_{i=N-2}^{N-j}\mathbf{V}_i^{-T}\mathbf{a}_L + \prod_{i=N-2}^{0}\mathbf{V}_i^{-T}\mathbf{b}_L & = & \mathbf{0}_L,
\end{array}$$

IV. Lattice Parameterization

In this section, a lifting structure is used to parameterize non-singular matrices $\mathbf{U}_0$ and $\mathbf{V}_i$. This structure has several advantages over the direct and the SVD structures as discussed later in this section.

Lemma 1: Any non-singular $L \times L$ matrix $\mathbf{A}$ can be decomposed as:

$$\mathbf{A} = \mathbf{RDLP},$$

where

$$\mathbf{R} = \begin{bmatrix} 1 & r_1 & \cdots & r_{L-1} \\ & 1 & & \\ & & \vdots & \\ & & \cdots & 1 \end{bmatrix}, \quad \mathbf{L} = \begin{bmatrix} 1 & & \cdots & \\ \ell_1 & & & \\ & & \vdots & \\ \ell_{L-1} & & \cdots & 1 \end{bmatrix},$$

and $\mathbf{D} = \begin{bmatrix} \alpha & \\ & \overline{\mathbf{A}} \end{bmatrix}$ is non-singular, i.e. $\overline{\mathbf{A}}$ is non-singular and $\alpha \neq 0$. Figure 4 illustrates the parameterization of this matrix $\mathbf{A}$. The matrix $\mathbf{P}$ is a permutation matrix which switches between the first row and a certain i-th row i. For example, for $i = 3$, we have

$$\mathbf{P} = \begin{bmatrix} 0 & 0 & \cdots & 1 & \cdots & 0 \\ 0 & 1 & \cdots & 0 & \cdots & 0 \\ & & \vdots & & & \\ 1 & 0 & \cdots & 0 & \cdots & 0 \\ & & \vdots & & & \\ 0 & 0 & \cdots & 0 & \cdots & 1 \end{bmatrix}$$

as shown in Figure 5.

Counting the number of free parameters of $\mathbf{A}$, we can see that $\mathbf{R}$ and $\mathbf{L}$ have up to $2(L-1)$ nonzero lifting coefficients. The matrix $\mathbf{D}$ has one nonzero multiplication and a $(L-1)\times(L-1)$ matrix $\overline{\mathbf{A}}$ which can be parameterized by another $(L-1)^2$ parameters. Hence the total number of the free parameters of $\mathbf{A}$ is $1+2(L-1)+(L-1)^2 = L^2$, which is equal to that obtained from the direct parameterization or the SVD factorization. Thus this factorization is minimal in the sense that the number of free parameters is minimized.

The proposed lifting structure provides many advantages over the direct and SVD structures. First, let us compare this to the direct structure. The new lifting structure offers a robust implementation of the matrix $\mathbf{A}$ with integer coefficients, i.e., the coefficients r_i and ℓ_i can be quantized in both $\mathbf{A}$ and $\mathbf{A}^{-1}$ and the quantized versions still preserve invertibility between them. The entire matrix $\mathbf{A}$ and its inverse can also be obtained with all integer coefficients if the same structure is repeated in $\overline{\mathbf{A}}$ and so on. On the other hand, in the direct structure, if the elements of $\mathbf{A}$ and $\mathbf{A}^{-1}$ are quantized directly, invertibility is no longer guaranteed.

Now, let us explore the above with the SVD structure, which is a product of two orthogonal matrices and a diagonal matrix in between. Each orthogonal matrix can be implemented using $\binom{L}{2}$ rotation angles. Each angle can be implemented using a butterfly with four floating point multiplications ($\sin\theta$ and $\cos\theta$). The integer implementation is also possible by converting each butterfly into three lifting steps and these lifting coefficients can be quantized with invertibility preserved. Each lifting is equivalent to one multiplication and therefore, for an $L\times L$ matrix, there are $2\times\binom{L}{2}\times 3+L = 3L^2-2L$ multiplications. On the other hand, in the new lifting structure, each lifting is equivalent to one multiplication and thus the number of multiplications is only L^2. Hence, this new structure is also more efficient from a computational complexity standpoint.

In the remaining of this section, a new method for imposing regularities into a BOLP filter bank is discussed where each invertible matrix is parameterized using the above lifting structure. In particular, we shall demonstrate that one and two vanishing moments can be imposed directly onto the parameters ℓ_i, r_i and α of the free-parameter matrices $\mathbf{U}_0$ and $\mathbf{V}_i$.

A. (1,1)-Regular Systems

For BOLP systems, the degree of regularity or the number of vanishing moments of the analysis and synthesis lowpass filters are not equal in general, and thus imposing a number of zeros at DC of the bandpass and highpass analysis filters does not imply that the synthesis bandpass and highpass filters will have the same number of zeros at DC. In fact, this is equivalent to imposing the same number of zeros at mirror frequencies of the synthesis lowpass filter.

Condition A_{01} requires the analysis bandpass and highpass filters to have zero response at DC, i.e., $F_0(z)$ has regularity of degree one. This condition can be satisfied by constraining the sum of the elements in each row of $\mathbf{U}_0$, except for the first one, to be zero. Similarly, condition A_{10} is equivalent to the fact that the synthesis bandpass and highpass filters have zero responses at DC, i.e., $H_0(z)$ is 1-regular. It is easy to show that conditions A_{01} and A_{10} together imply that $c_0 d_0 = L$. Therefore, in order to satisfy both conditions, all elements of the first row of $\mathbf{U}_0$ must be c_0/L. This is consistent with the result in the PU case where $\mathbf{U}_0^{-T} = \mathbf{U}_0$: hence $L/c_0 = c_0$, implying that $c_0 = \sqrt{L}$. In the case of BOLP filter banks, if the first row of the matrix is a constant vector, the sum of the elements in each other row is zero as it is orthogonal to the first row. Therefore only one of the two conditions is sufficient to enforce the first degree of regularity in both analysis and synthesis bank, provided that $d_0 = \frac{L}{c_0}$.

In order to parameterize $\mathbf{U}_0$, let us decompose $\mathbf{U}_0$ using the structure presented in Figure 4, i.e.,

$$\mathbf{U}_0 = \mathbf{RDLP}.$$

Since $\mathbf{P1}_L = \mathbf{1}_L$, it is easy to see that the first vanishing moment of the analysis and synthesis bandpass/highpass filters does not depend on the choice of $\mathbf{P}$.

Theorem 2: The conditions A_{01} and A_{10} can be simultaneously satisfied by choosing

$$\ell_1 = \ell_2 = \cdots = \ell_{L-1} = -1, \quad \alpha = c_0 \quad \text{and} \quad \mathbf{r} = \frac{c_0}{L}\overline{\mathbf{U}}_0^{-T}\mathbf{1}_{L-1}.$$

where $\mathbf{r} = [r_1 \; r_2 \; \cdots \; r_{L-1}]^T$.

Proof: When all analysis bandpass and highpass filters have zero magnitude response at DC, we have $\mathbf{U}_0\mathbf{1}_L = \mathbf{RDLP1}_L = \mathbf{RDL1}_L = c_0\mathbf{a}_L$. Hence, $\mathbf{L1}_L = c_0\mathbf{D}^{-1}\mathbf{R}^{-1}\mathbf{a}_L = c_0\mathbf{D}^{-1}\mathbf{a}_L = \frac{c_0}{\alpha}\mathbf{a}_L$, which implies that $\alpha = c_0$ and $\ell_i = -1$. Now let us assume that the synthesis bandpass and highpass filters also have zero magnitude response at DC, i.e.,

$$\mathbf{U}_0^{-T}\mathbf{1}_L = \mathbf{R}^{-T}\mathbf{D}^{-T}\mathbf{L}^{-T}\mathbf{P1}_L = \mathbf{R}^{-T}\mathbf{D}^{-T}\mathbf{L}^{-T}\mathbf{1}_L = d_0\mathbf{a}_L.$$

Therefore,

$$\begin{aligned} d_0\mathbf{R}^T\mathbf{a}_L = \mathbf{D}^{-T}\mathbf{L}^{-T}\mathbf{1}_L &= \mathbf{D}^{-T}\begin{bmatrix} L \\ \mathbf{1}_{L-1} \end{bmatrix} \\ &= d_0\begin{bmatrix} 1 \\ \mathbf{r} \end{bmatrix}\begin{bmatrix} L/\alpha \\ \overline{\mathbf{U}}_0^{-T}\mathbf{1}_{L-1} \end{bmatrix}, \end{aligned}$$

leading to $d_0 = \frac{L}{\alpha} = \frac{L}{c_0}$ and $\mathbf{r} = \frac{1}{d_0}\overline{\mathbf{U}}_0^{-T}\mathbf{1}_{L-1} = \frac{c_0}{L}\overline{\mathbf{U}}_0^{-T}\mathbf{1}_{L-1}$. □

Example 1: In this design example, a (1,1)-regular 16-tap 8-channel BOLP filter bank is designed using the proposed theory. The frequency responses, the zeros of the lowpass filters, and the corresponding scaling and wavelet functions of both analysis and synthesis bank are shown in Figure 6.

B. (1,2)-Regular Systems

We can follow the method in the previous case, assuming that both $H_0(z)$ and $F_0(z)$ have at least one regularity, i.e., the conditions A_{01} and A_{10} are satisfied. To obtain a (1,2)-regular system, we have to impose another degree of regularity into $F_0(z)$. This is equivalent to the analysis bandpass and highpass filters having two zeros at DC (second vanishing moment). In term of the lattice components, this is condition A_{02}. Note that this condition is exactly the same as that in the PU case [18] except that, here, the matrices $\mathbf{U}_i$ and $\mathbf{V}_i$ are non-singular, and the condition A_{02} does not imply a second vanishing moment for the synthesis bank.

For convenience, let

$$\mathbf{c} = -c_0\left(\mathbf{I} + \sum_{j=3}^{N-1}\prod_{i=N-3}^{N-j}\mathbf{V}_i\right)\mathbf{a}_L - \left(\prod_{i=N-3}^{0}\mathbf{V}_i\right)\mathbf{b}_L.$$

Hence the condition A_{02} can be simplified to

$$\mathbf{V}_{N-2}\mathbf{c} = c_0\mathbf{a}_L. \tag{5}$$

Assuming that $\mathbf{V}_i$ for $i < N-2$ are known, $\mathbf{c}$ is also known. Let us parameterize $\mathbf{V}_{N-2}$ as in Figure 4. The condition (5) can be satisfied by choosing the lifting parameters ℓ_i and α in Figure 4 as in the following theorem.

Theorem 3: Let $\tilde{\mathbf{c}} = \mathbf{Pc}$. $\mathbf{V}_{N-2}$ satisfies (5) if and only if

$$\alpha = \frac{c_0}{\tilde{c}_1} \quad \text{and} \quad \ell_i = -\frac{\tilde{c}_{i+1}}{\tilde{c}_1}, \quad \text{for } i = 1, \cdots, L-1,$$

where $\tilde{\mathbf{c}} = [\tilde{c}_1 \; \tilde{c}_2 \; \cdots \; \tilde{c}_{L-1}]^T$.

Proof: Assume that (5) holds, we have

$$\mathbf{V}_{N-2}\mathbf{c} = \mathbf{RDLPc} = \mathbf{RDL}\tilde{\mathbf{c}} = \sqrt{L}\mathbf{a}_L.$$

Hence

$$\begin{aligned} &[\tilde{c}_1 \quad \tilde{c}_2 + \ell_1\tilde{c}_1 \quad \tilde{c}_3 + \ell_2\tilde{c}_1 \quad \cdots \quad \tilde{c}_L + \ell_{L-1}\tilde{c}_1\,]^T \\ &= \mathbf{L}\tilde{\mathbf{c}} = \sqrt{L}\mathbf{D}^{-1}\mathbf{R}^{-1}\mathbf{a}_L = \sqrt{L}\mathbf{D}^{-1}\mathbf{a}_L = \alpha\sqrt{L}\mathbf{a}_L, \end{aligned}$$

which completes the proof. □

Example 2: In this design example, a (1,2)-regular 8-tap 4-channel BOLP filter bank is designed using the proposed theory. The frequency responses, the time responses, and the corresponding scaling and wavelet functions of both analysis and synthesis banks are shown in Figure 7 where the enhanced smoothness in the synthesis bank is evident. Note that we purposely choose rational parameters in this design. The detailed rational-coefficient lattice is depicted in Figure 8.

Example 3: In this design example, a (1,2)-regular 16-tap 8-channel BOLP filter bank is designed using the proposed theory. The frequency responses, the zeros of the lowpass filters, and the corresponding scaling and wavelet functions of the analysis and synthesis banks are shown in Figure 9.

C. (2,2)-regular systems

In this section, we impose the second vanishing moment into both analysis and synthesis filter banks. To begin, recall that the filter bank is (2,2)-regular then the condition A_{22} must be satisfied. Let

$$\mathbf{c} = -c_0\left(\mathbf{I} + \sum_{j=3}^{N-1}\prod_{i=N-3}^{N-j}\mathbf{V}_i\right)\mathbf{a}_L + \left(\prod_{i=N-3}^{0}\mathbf{V}_i\right)\mathbf{b}_L$$

$$\mathbf{d} = -\frac{L}{c_0}\left(\mathbf{I} + \frac{L}{c_0}\sum_{j=3}^{N-1}\prod_{i=N-3}^{N-j}\mathbf{V}_i^{-T}\right)\mathbf{a}_L + \left(\prod_{i=N-3}^{0}\mathbf{V}_i^{-T}\right)\mathbf{b}_L.$$

The above conditions can be imposed into one of the $N-1$ matrices $\mathbf{V}_i$, $i \le N-2$, if the other $N-2$ matrices $\mathbf{V}_i$ are known. Without loss of generality, let us assume that the matrices $\mathbf{V}_i$ are chosen in the increasing order. The above conditions can be rewritten as

$$\mathbf{V}_{N-2}\mathbf{c} = c_0\mathbf{a}_L \quad (6)$$

$$\mathbf{V}_{N-2}^{-T}\mathbf{d} = \frac{L}{c_0}\mathbf{a}_L. \quad (7)$$

It is easy to show that both (6) and (7) hold only if

$$\mathbf{d}^T\mathbf{c} = (\mathbf{d}^T\mathbf{V}_{N-2}^{-1})(\mathbf{V}_{N-2}\mathbf{c}) = \left(\frac{L}{c_0}\mathbf{a}^T\right)(c_0\mathbf{a}) = L. \quad (8)$$

Clearly, this condition is independent of the choice of $\mathbf{V}_i$ for $i \geq N-2$. When $N=2$, $\mathbf{c}=\mathbf{d}=\mathbf{b}_L$ and hence $\mathbf{d}^T\mathbf{c} = \|\mathbf{b}_L\|^2 \neq L$ which proves that the filter length of a (2,2)-regular filter bank is at least $3M$ – a similar result to that of the PU case [19]. When $N \geq 3$, the above scalar algebraic equation can be imposed into one of the matrices $\mathbf{V}_i$ with $i \leq N-3$. Since the matrices $\mathbf{V}_i$ are determined in the increasing order, this condition can be imposed onto $\mathbf{V}_{N-3}$ after $\mathbf{V}_i$ for $i < N-3$ are known. Let

$$\hat{\mathbf{c}} = -c_0\left(\mathbf{I} + \sum_{j=4}^{N-1}\prod_{i=N-4}^{N-j}\mathbf{V}_i\right)\mathbf{a}_L + \left(\prod_{i=N-4}^{0}\mathbf{V}_i\right)\mathbf{b}_L, \quad \text{and}$$

$$\hat{\mathbf{d}} = -\frac{L}{c_0}\left(\mathbf{I} + \frac{L}{c_0}\sum_{j=4}^{N-1}\prod_{i=N-4}^{N-j}\mathbf{V}_i^{-T}\right)\mathbf{a}_L + \left(\prod_{i=N-4}^{0}\mathbf{V}_i^{-T}\right)\mathbf{b}_L,$$

then (8) becomes

$$\frac{L}{c_0}\mathbf{a}_L^T\mathbf{V}_{N-3}\hat{\mathbf{c}} + c_0\hat{\mathbf{d}}^T\mathbf{V}_{N-3}^{-T}\mathbf{a}_L + \hat{\mathbf{c}}^T\hat{\mathbf{d}} = 0. \quad (9)$$

Let $\mathbf{V}_{N-3}$ be parameterized as in Figure 4. After some manipulation, one can show that

$$\frac{L}{c_0}[\alpha + \mathbf{r}^T\overline{\mathbf{V}}_{N-3}\ell \;\; \mathbf{r}^T\overline{\mathbf{V}}_{N-3}]\mathbf{P}\hat{\mathbf{c}} + \frac{c_0}{\alpha}\mathbf{d}^T\mathbf{P}\begin{bmatrix} 1 \\ \ell \end{bmatrix} + \hat{\mathbf{c}}^T\hat{\mathbf{d}} = 0. \quad (10)$$

It is easy to show that this equation can be easily imposed into one of the liftings r_i and ℓ_i of $\mathbf{V}_{N-3}$ as it forms a linear equation of each of these parameters. One can also impose this into α, however, the equation becomes quadratic and it is possible for α to be complex for some choices of r_i and ℓ_i.

Theorem 4: Assume that conditions A_{01} and A_{10} hold and (10) is satisfied. For any choices of $\mathbf{U}_0$ and $\mathbf{V}_i$ ($i < N-2$), the resulting filter bank is (2,2)-regular if and only if the following conditions hold:

1. $\alpha = \frac{\sqrt{L}}{\tilde{c}_1}$.
2. $\ell_i = -\frac{\tilde{c}_{i+1}}{\tilde{c}_1}$ for $i = 1, \cdots, L-1$.
3. $[r_1 \; r_2 \; \cdots \; r_{L-1}] = \frac{\alpha}{\tilde{d}_1}[\tilde{d}_2 \; \tilde{d}_3 \; \cdots \; \tilde{d}_L]\overline{\mathbf{V}}_{N-2}^{-1}$.

Proof: The conditions 1 and 2 are exactly the same as that in Theorem 3. From (7), we have

$$\mathbf{V}_{N-2}^{-T}\mathbf{d} = \mathbf{R}^{-T}\mathbf{D}^{-T}\mathbf{L}^{-T}\mathbf{P}\mathbf{d} = \mathbf{R}^{-T}\mathbf{D}^{-T}\mathbf{L}^{-T}\tilde{\mathbf{d}} = \frac{L}{c_0}\mathbf{a}_L.$$

Hence

$$\frac{L}{c_0}\mathbf{R}^T\mathbf{a}_L = \frac{L}{c_0}[1 \; r_1 \; \cdots \; r_{L-1}]^T = \begin{bmatrix} \beta \\ \overline{\mathbf{V}}_{N-2}^{-T}[\tilde{d}_2 \; \tilde{d}_3 \; \cdots \tilde{d}_L]^T \end{bmatrix}$$

for some β. It is easy to show that with the choice of $\mathbf{V}_{N-3}$ in (10), $\beta = L/c_0$ and thus the proof is complete. □

Example 4: In this design example, a (2,2)-regular 24-tap 8-channel BOLP filter bank is designed using the proposed theory. The frequency responses, the zeros of the lowpass filters, and the corresponding scaling and wavelet functions of the analysis and synthesis banks are shown in Figure 10.

V. Coding Examples

In this section, the regular filter banks obtained from several design examples presented in previous sections are used in an image compression application. The progressive image transmission algorithm (block transform + regrouping coefficients + zero-tree coding) is used to compare the performances of the transforms. For more details on progressive image transmission, the reader is referred to [20], [21]. The BOLP filter banks are used as block transforms in the progressive image transmission, and the performances are compared with that obtained by using other existing PULP filter banks.

Tables I and II summarize the properties of each transform used in the simulation and the PSNR of the reconstruction images. Boldfacing highlights the maximum PSNR at each compression ratio. According to Table II, the maximum PSNR at compression ratios of 8, 16, 32 and 100 to 1 are obtained when the 8-channel 24-tap 1-regular PULP filter bank is used. At 64 to 1, the 8-channel 16-tap (1,1)-regular BOLP filter bank has the highest PNSR, and the 8-channel 16-tap (1,2)-regular BOLP filter bank yields the best PSNR at 128 to 1. Figure 11 shows enlarged reconstructed portions of the Barbara image at compression ratio of 64 to 1 using different transforms. It is evident that the images reconstructed by the DCT, LOT and PULPv1 suffer from the blocking artifact. Though the reconstructions from the PULPv2 and BOLPv11 yield better perceptual qualities, some of the texture details are eliminated. The reconstruction using the BOLPv12 yields the best perceptual quality since most of the textures are preserved while there is no severe blocking artifact on smooth regions.

VI. Conclusion

In this paper, we have presented a method for imposing regularity properties onto BOLP filter banks. A new lattice structure for parameterizing a non-singular matrix via lifting steps is presented. This new structure has several advantages over the conventional direct and SVD parameterizations in terms of number of free parameters and robustness to the quantization of the lifting coefficients. Regarding regular filter banks, we consider three cases of (1,1), (1,2) and (2,2)-regular systems where the corresponding permissible minimal filter lengths are M, $2M$, and $3M$

respectively. By using the proposed parameterization of non-singular matrices, the conditions for regularity of the filter banks can be imposed with ease into the lifting steps. Finally, these transforms are tested in an image coding application, and shown to outperform the conventional PULP filter banks.

Appendix

I. Proof of Proposition 1

1. We shall prove by using the modulation matrices $\mathbf{H}_m(z)$ and $\mathbf{F}_m(z)$ whose (i,j) elements are $H_i(W^j)$ and $F_i(W^j)$ where $W = e^{j2\pi/M}$. First, let us prove the first statement by induction on K_s. Recall that the PR property of the filter bank yields

$$\mathbf{F}_m(z)\mathbf{H}_m^T(z) = \text{a diagonal matrix.} \tag{11}$$

(a) $\underline{K_s = 1}$. Assume that $F_0(W^j) = 0$ for all $j = 1, 2, ..., M-1$. Substituting $z = 1$ into (11) yields

$$\sum_j F_0(W^j)H_j(W^i) = 0$$

for all $i > 0$. Hence $H_i(1) = 0$.
(b) $\underline{K_s = n}$. Assume that the first statement of the theorem is true for $K_s < n$. It is now sufficient to show that if $F_0(z)$ has n multiple zeros at aliasing frequencies W^j for all $j > 0$ then $H_i(z)$ have n multiple zeros at DC frequency. Suppose that $F_0(z)$ has n zeros at W^j for all $j > 0$, in order to show that the bandpass/highpass filters $H_i(z)$ have n zeros at DC for all $i > 0$, it suffices to show that $H_i(z)$ are of the form $H_i(z) = (1 - z^{-1})^n Q_i(z)$ where $Q_i(z)$ are some polynomials (since all the filters are FIR) in z^{-1}. Equivalently, the r^{th} derivative of $H_i(z)$ with respect to z^{-1} and evaluated at $z = 1$ is zero for all $r = 0, 1, ..., n-1$. Repeatedly applying the derivative operator $n-1$ times to (11) with respect to z^{-1} implies that

$$\sum_{\ell=0}^{n-1} \binom{n-1}{\ell} \left[\mathbf{F}_m(z)\right]^{(\ell)} \left[\mathbf{H}_m^T(z)\right]^{(n-1-\ell)} = \text{ diagonal matrix.} \tag{12}$$

After substituting $z = 1$, we can rewrite (12) as Consider the off-diagonal elements of the first column of $[\mathbf{F}_m(z)]^{(\ell)} \left[\mathbf{H}_m^T(z)\right]^{(n-1-\ell)} |_{z=1}$. Since $F_0(z)$ has n zeros at all aliasing frequencies, the off-diagonal elements of the first row in $[\mathbf{F}_m(z)]^{(\ell)} |_{z=1}$ are zero for $\ell = 0, 1, ..., n-1$. By the assumption of induction, the off-diagonal elements of the first row in $[\mathbf{H}_m(z)]^{(n-1-\ell)} |_{z=1}$ are zero for $\ell = 1, 2, ..., n-1$ which imply that the off-diagonal elements of the first row in $[\mathbf{F}_m(z)] \left[\mathbf{H}_m^T(z)\right]^{(n-1)} |_{z=1}$ must be zero, i.e.

$$\sum_j \left[F_0(W^j z)\right] \left[H_k(W^j z)\right]^{(n-1)} |_{z=1} = 0, \tag{14}$$

for $k = 1, 2, ..., M$. Hence $[H_k(z)]^{(n-1)} |_{z=1} = 0$ for all $k > 0$ which completes the proof. The second statement can be proven in the same manner by noting that

$$\mathbf{F}_m^T(z)\mathbf{H}_m(z) = \text{ diagonal matrix,} \tag{15}$$

and will be left as a simple exercise for the reader.

2. We will show only for the case of (a) since the two conditions are analogous. The proof is straight forward from the fact that $H_i(z)$ has K_s zeros at DC. Let us write $H_i(z)$ as

$$H_i(z) = \sum_n h_i(n)z^{-n} = (z-1)^{K_s} Q^0(z), \tag{16}$$

where $Q^0(z)$ is some function of z such that $Q^0(1) \neq 0$. Hence

$$\sum_n h_i(n) = H_i(1) = 0.$$

Now let us differentiate (16) with respect to z we get

$$-\sum_n nh_i(n)z^{-n-1} = (z-1)^{K_s-1}[K_s Q^0(z) + (z-1)\frac{d}{dz}Q^0(z)].$$

Let $Q^1(z) = -z[K_s Q^0(z) + (z-1)\frac{d}{dz}Q^0(z)]$, then

$$\sum_n nh_i(n)z^{-n} = (z-1)^{K_s-1}Q^1(z). \tag{17}$$

It is clear that if $K_s > 1$, substituting $z = 1$ into (17) implies (a) for $n = 1$. For $n = 2, \cdots, K_s$, successively differentiating and substituting $z = 1$ as above complete the proof.
3. We will only prove for $\psi_i(t)$. From the definition of $\psi_i(t)$ for $i > 0$, we have

$$\begin{aligned}
\int t^j \psi_i(t)dt &= \int t^j \sum_k h_i(k)\phi(Mt-k)dt \\
&= \int \sum_k t^j h_i(k)\phi(Mt-k)dt \\
&= \int \sum_k \left(\frac{\tau+k}{M}\right)^j h_i(k)\phi(\tau)\frac{d\tau}{M} \\
&= \frac{1}{M^{j+1}} \int \phi(\tau) \sum_k \sum_{\ell=0}^{j} \binom{j}{\ell} \tau^{j-\ell}k^\ell h_i(k)d\tau \\
&= \frac{1}{M^{j+1}} \int \phi(\tau) \sum_{\ell=0}^{j} \binom{j}{\ell} \tau^{j-\ell} \sum_k k^\ell h_i(k)d\tau
\end{aligned}$$

From 2., if $j \leq K_s$, the ℓ^{th} moment of $h_i(k)$ in the last equation is zero because $\ell \leq j \leq K_s$, and hence $\int t^j w_i(t)dt = 0$ as desired.

4. We will integrate by part the quantity in the absolute value. Let $I^1(t) = \int_{-\infty}^{t} \widetilde{\psi}_i(\tau)d\tau$ hence $\widetilde{\psi}_i(M^j t - k)dt = M^{-j}dI^1(M^j t - k)$. From 3., it is clear that $I^1(\infty) = 0$. In fact $I^1(t)$ has the same compact support as $\widetilde{\psi}_i(t)$. Therefore

$$\int g(t)\widetilde{\psi}_i(M^j t - k)dt = -M^{-j} \int g'(t)I^1(M^j t - k)dt. \tag{18}$$

$$\left[\mathbf{F}_m(z)\right]\left[\mathbf{H}_m^T(z)\right]^{(n-1)}\Big|_{z=1}+\sum_{\ell=1}^{n-1}\binom{n-1}{\ell}\left[\mathbf{F}_m(z)\right]^{(\ell)}\left[\mathbf{H}_m^T(z)\right]^{(n-1-\ell)}\Big|_{z=1}= \text{ diagonal matrix.} \tag{13}$$

Again, let $I^2(t)=\int_{-\infty}^t I^1(\tau)d\tau=\int_{-\infty}^t\int_{-\infty}^{\tau}\widetilde{\psi}_i(s)dsd\tau$. Integrating by parts the above equation yields

$$\begin{aligned} I^2(t) &= \tau I^1(\tau)\big|_{-\infty}^t-\int_{-\infty}^t \tau dI^1(\tau) \\ &= \tau I^1(\tau)\big|_{-\infty}^t-\int_{-\infty}^t \tau\widetilde{\psi}_i(\tau)d\tau. \end{aligned}$$

Hence $I^2(\infty)=0$ and (18) becomes

$$\int g(t)\widetilde{\psi}_i(M^jt-k)dt=M^{-2j}\int g''(t)I^2(M^jt-k)dt. \tag{19}$$

Repeating the same procedure yields

$$\begin{aligned} \left|\int g(t)\widetilde{\psi}_i(M^jt-k)dt\right| &= \left|M^{-jK_s}\int g^{(K_s)}(t)I^{K_s}(M^jt-k)dt\right| \\ &\le CM^{-jK_s}\|g^{(K_s)}(t)\|. \end{aligned}$$

5. The proof is directly from the orthogonality between $\phi(t)$ and $\widetilde{\psi}_i(t)$.
6. We will prove by induction on K_s similar to the case of $M=2$ in [1]. It is obvious that when $K_s=1$, 1 is an eigenvalue of $\mathbf{L}$. Now assuming that $\ell_{old}\mathbf{x}_{old}=\lambda_{old}\mathbf{x}_{old}$ which is equivalent to

$$\sum_{k=0}^{M-1}H_0(W^kz)X(W^kz)=\lambda X(z^M).$$

$$\begin{aligned} &\left(\frac{1-z^M}{M}\right)\sum_{k=0}^{M-1}H_0(W^kz)X(W^kz) \\ &=\sum_{k=0}^{M-1}\left\{\frac{1+W^kz+\cdots+(W^kz)^{M-1}}{M}\right\}H(W^kz)(1-W^kz)X(W^kz) \\ &=\sum_{k=0}^{M-1}H_{new}(W^kz)(1-W^kz)X(W^kz) \\ &=\sum_{k=0}^{M-1}H_{new}(W^kz)X_{new}(W^kz) \end{aligned}$$

$$\left(\frac{1-z^M}{M}\right)X(z^M)=\frac{\lambda}{M}X_{new}(z^M)$$

Hence $\lambda_{new}=\frac{\lambda_{old}}{M}$. The extra eigenvalue 1 comes from the first regularity. If $H(z)$ has a factor $(1+z^{-1}+\cdots+z^{1-M})$, then $\sum_k h(Mk+j)=\frac{1}{M}$ for all j and hence Therefore 1 is an eigenvalue with the corresponding left-eigenvector $[1\ 1\ \cdots\ 1]$.

TABLE I
OBJECTIVE PROPERTIES OF THE FILTER BANKS.

Transform	Coding gain(dB)	Regularity	Stopband attn. (-dB)
8×8 DCT	8.83	1	4.43
8×16 LOT	9.22	1	16.32
8×24 PULPv1	9.36	1	19.48
8×24 PULPv2	9.33	2	13.00
8×16 BOLPv11	**9.62**	(1,1)	13.76
8×16 BOLPv12	9.60	(1,2)	12.53

REFERENCES

[1] G. Strang and T. Nguyen. *Wavelets and Filter Banks.* Wellesley-Cambridge, Wellesley, MA, 1996.
[2] K.R. Rao and J.J. Hwang. *Techniques and Standards for Image, Video, and Audio Coding.* Prentice-Hall, Englewood Cliffs, NJ, 1996.
[3] FBI Criminal Justice Informaction Services. Wavelet scalar quantization gray scale fingerprint image compression specification, 1993.
[4] K. Sayood. Introduction to data compression, 2000.
[5] H.S. Malvar. *Signal Processing with Lapped Transforms.* Artech House, Norwood, MA, 1992.
[6] R.L. de Queiroz, T.Q. Nguyen, and K.R. Rao. The genlot: Generalized linear-phase lapped orthogonal transform. *IEEE Trans. Signal Processing*, 44(3):497–507, March 1996.
[7] T. Tran, R. deQueiroz, and T. Nguyen. Linear-phase perfect reconstruction filter bank: lattice structure, design and application in image coding. *IEEE Trans. Signal Processing*, 48(1):133–147, January 2000.
[8] K.R. Rao and P. Yip. *Discrete Cosine Transform: Algorithms, Advantages, Applications.* Academic Press Inc., San Diego, CA, 1990.
[9] P.P. Vaidyanathan. *Multirate Systems and Filter Banks.* Prentice-Hall, Englewood Cliffs, NJ, 1993.
[10] I Daubechies. *Ten Lectures on Wavelets.* SIAM, 1992.
[11] P. Steffen, P.N. Heller, R.A. Gopinath, and C.S. Burrus. Theory of regular m-band wavelet bases. *IEEE Trans. Signal Processing*, 41(12):3497–3510, December 1993.
[12] S. Oraintara. *Regular Linear Phase Perfect Reconstruction Filter Banks for Image Compression.* PhD thesis, Boston University, month 2000.
[13] P.P. Vaidyanathan and A. Kirac. Results on optimal biorthogonal filter banks. *IEEE Trans. on Circuits and Systems II*, 45:932–947, 1998.
[14] T.D. Tran and T.Q. Nguyen. On m-channel linear-phase fir filter banks and application in image compression. *IEEE Trans. Signal Processing*, 45:2175–2187, September 1997.
[15] X.Q. Gao, T.Q. Nguyen, and G. Strang. The factorization of m-channel paraunitary filter banks. Submitted to IEEE Trans. Signal Processing, February 2000.
[16] E. Kreyszig. *Advanced Engineering Mathematics.* John Wiley & Sons, 8th edition, 1999.
[17] H. Zou and A.H. Tewfik. Discrete orthogonal m-band wavelet decompositions. *ICASSP*, 4:IV–605–IV–608, 1992.
[18] S. Oraintara, T. Tran, P. Heller, and T. Nguyen. Lattice structure for regular paraunitary linear phase filterbanks. *IEEE Trans. on Signal Processing*, 49(11):2659–2672, November 2001.
[19] S. Oraintara, P. Heller, T. Tran, and T. Nguyen. Lattice structure for regular-paraunitary linear-phase filter banks. In *Proc. 2nd International Workshop on Transforms and Filter Banks*, Brandenburg an der Havel, Germany, March 1999.
[20] A. Said and W.A. Pearlman. A new, fast, and efficient image codec based on set partitioning in hierarchical trees. *IEEE Trans. on Circuits and Systems for Video Technology*, 6(3):243–250, 1998.
[21] T.D. Tran and T.Q. Nguyen. A progressive transmission image coder using linear phase uniform filter banks as block transforms. *IEEE Trans. on Image Processing*, 48(11):1493–1507, November 1999.

$$M[1\ 1 \cdots 1]\begin{bmatrix} h(0) & & & & & \\ h(M) & h(M-1) & h(M-2) & \cdots & h(1) & h(0) \\ & h(2M-1) & h(2M-2) & \cdots & h(M+1) & h(M) \\ \vdots & \vdots & \vdots & \vdots & \vdots & \vdots \end{bmatrix} = [1\ 1 \cdots 1].$$

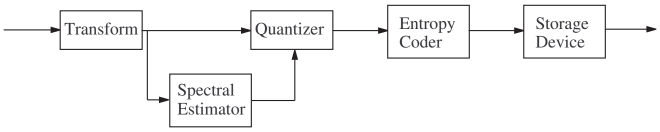

Fig. 1. A block diagram of image coder.

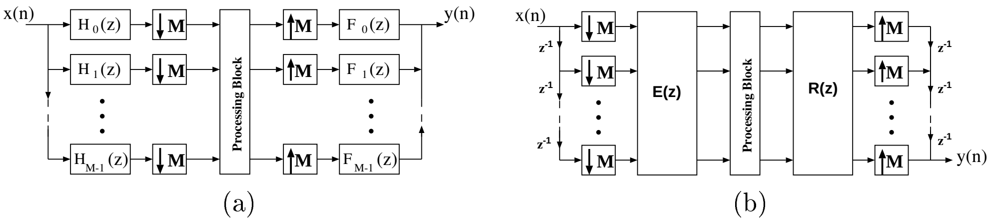

Fig. 2. An M-channel filter bank: (a) regular and (b) polyphase structures.

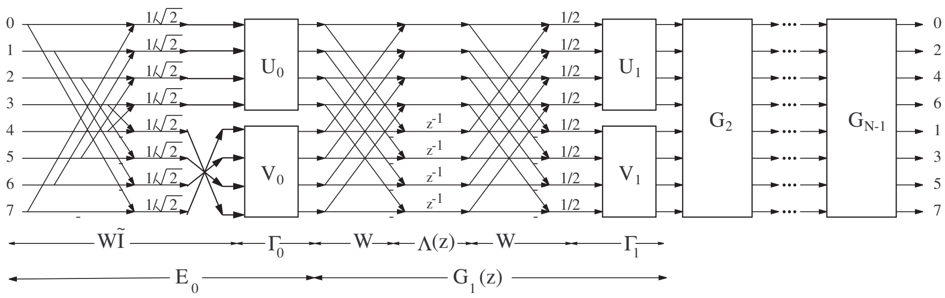

Fig. 3. Lattice structure for linear-phase lapped transform.

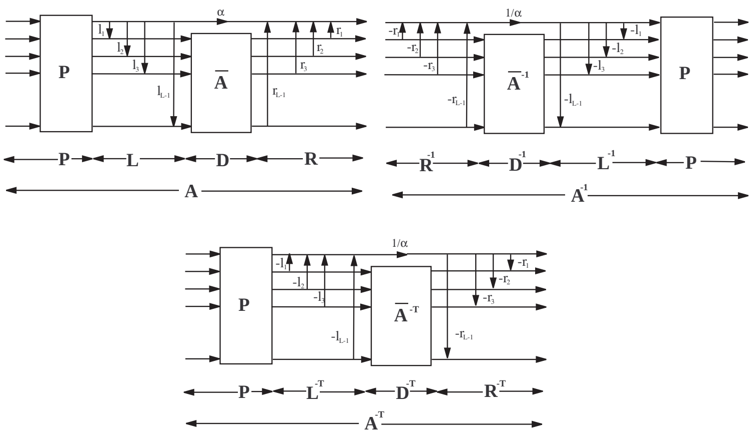

Fig. 4. Lifting parameterization of a non-singular matrix $\mathbf{A}$ and its inverse.

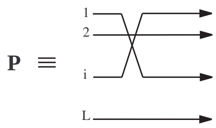

Fig. 5. Permutation matrix which switches between the first and the i^{th} elements.

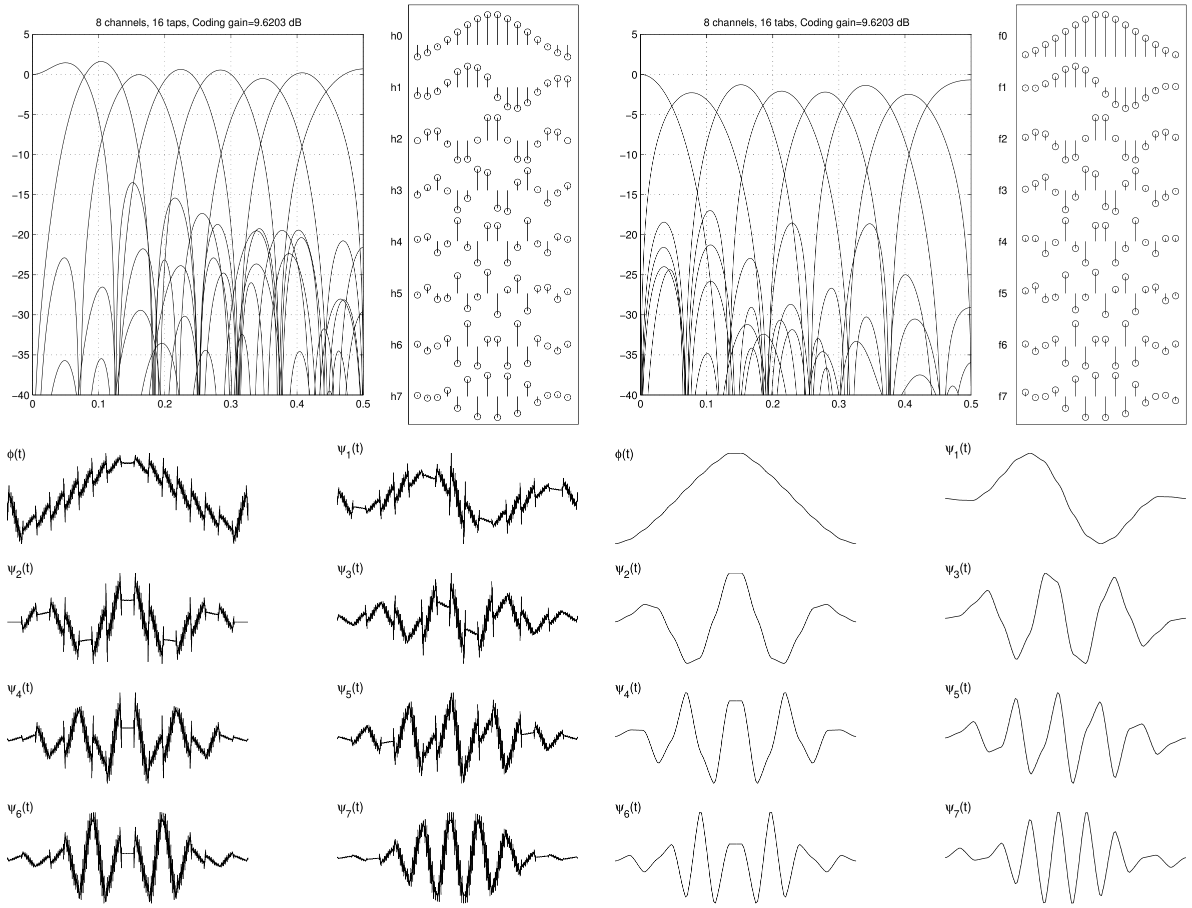

Fig. 6. A design example of (1,1)-regular 8-channel BOLP filter bank with length 16: frequency responses of the analysis (top-left) and synthesis (top-right) filters, and the scaling function and wavelets of the analysis (bottom-left) and synthesis (bottom-right) banks.

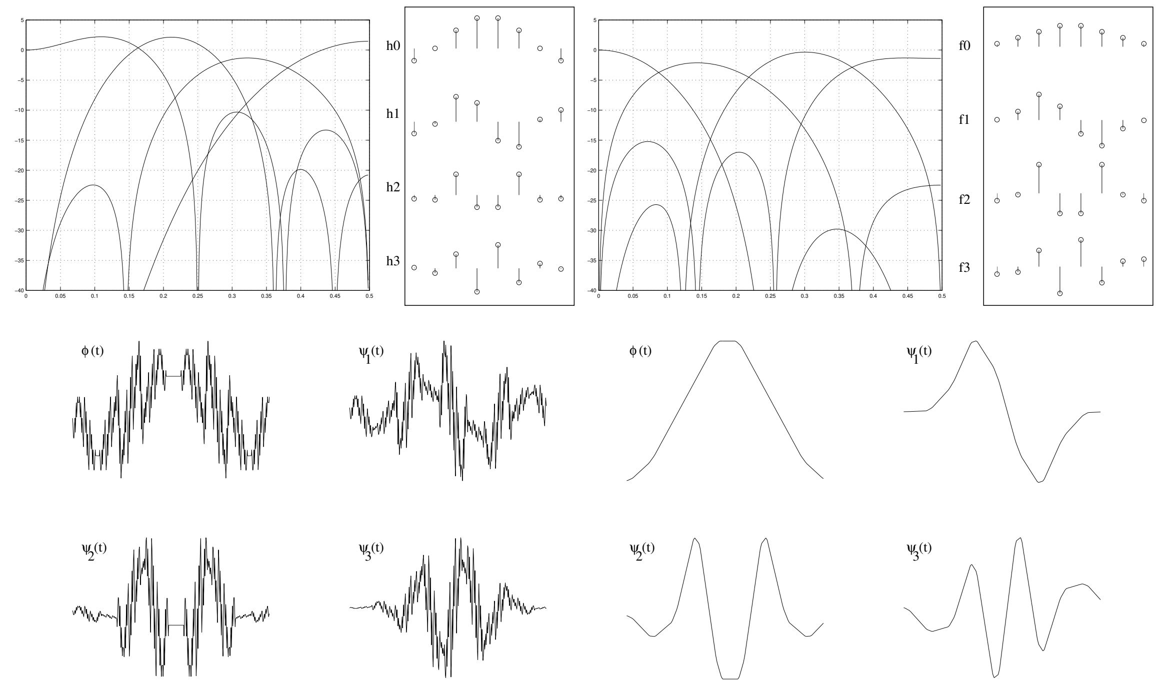

Fig. 7. A design example of (1,2)-regular 4-channel BOLP filter bank with length 8: frequency and time responses of the analysis filters (top-left); frequency and time responses of the synthesis filters (top-right); the scaling function and wavelets of the analysis (bottom-left) and synthesis (bottom-right) banks.

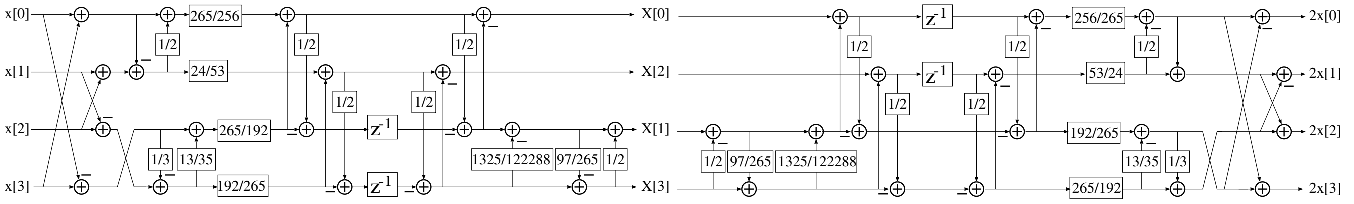

Fig. 8. Lattice structure of the (1,2)-regular 4-channel 8-tap rational-coefficient design example shown in Figure 7. Left: analysis bank. Right: synthesis bank.

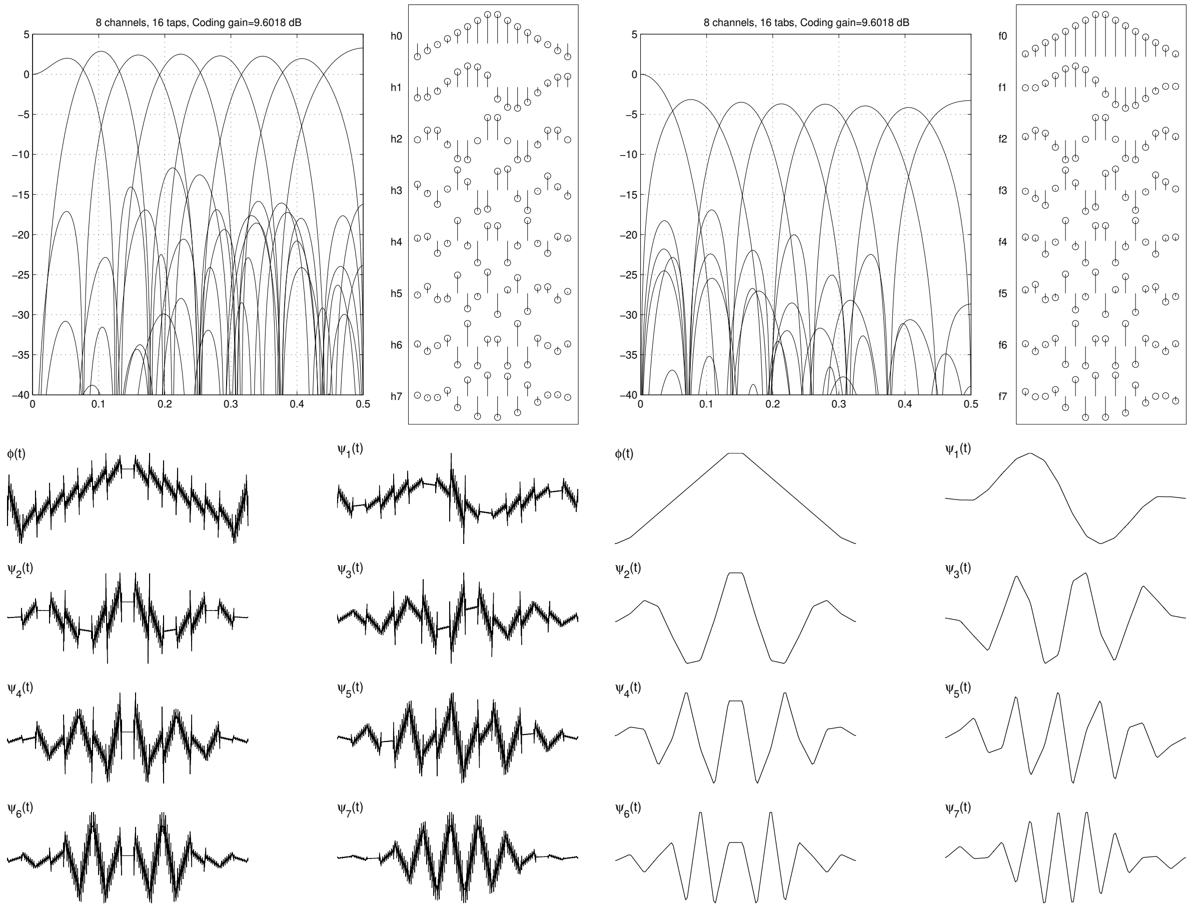

Fig. 9. A design example of (1,2)-regular 8-channel BOLP filter bank with length 16: frequency responses of the analysis (top-left) and synthesis (top-right) filters, and the scaling function and wavelets of the analysis (bottom-left) and synthesis (bottom-right) banks.

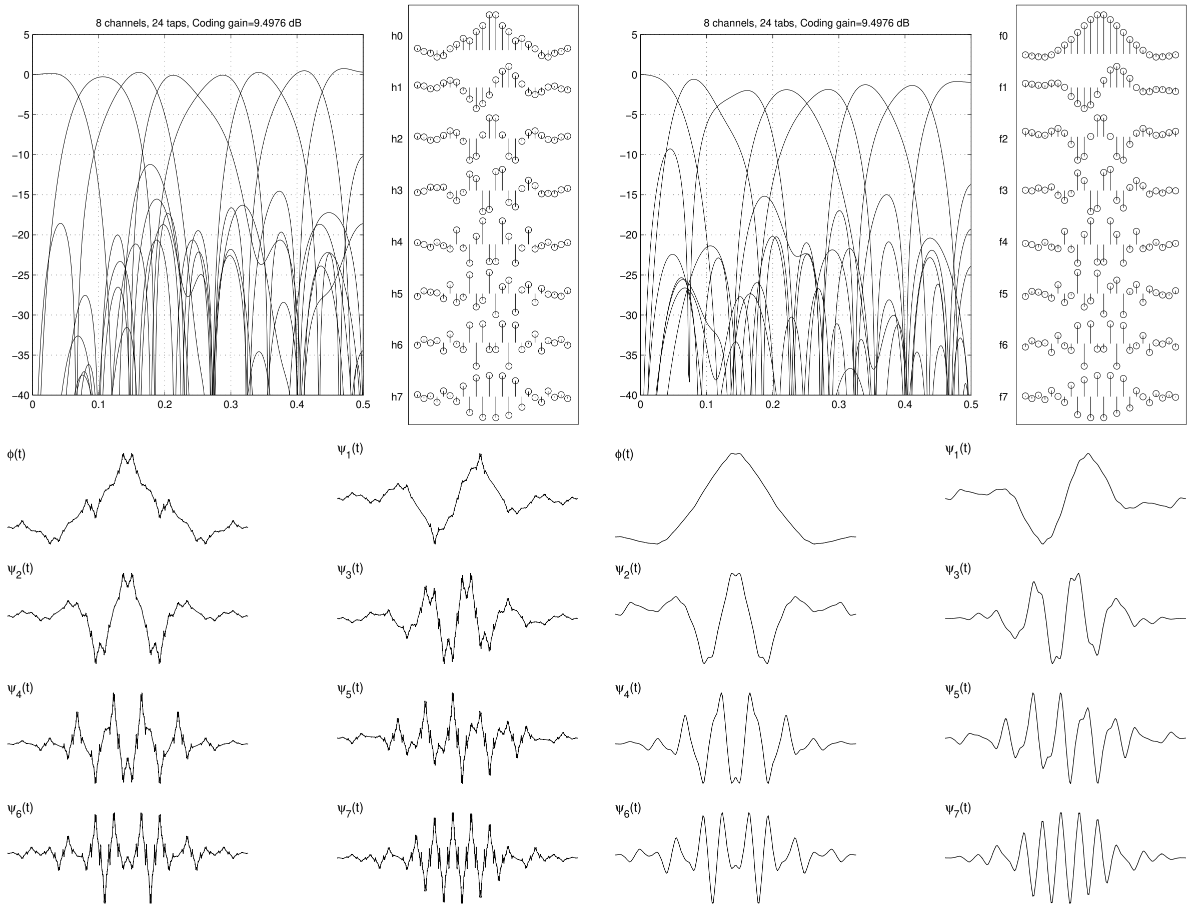

Fig. 10. A design example of (2,2)-regular 8-channel BOLP filter bank with length 24: frequency responses of the analysis (top-left) and synthesis (top-right) filters, and the scaling function and wavelets of the analysis (bottom-left) and synthesis (bottom-right) banks.

TABLE II
PSNR of the reconstructions using different LP filter banks.

	PSNR at different compression ratios (dB)					
Transform	1:8	1:16	1:32	1:64	1:100	1:128
SPIHT	36.41	31.40	27.58	24.86	23.76	23.35
8×8 DCT	36.31	31.11	27.28	24.58	23.42	22.68
8×16 LOT	37.43	32.70	28.80	25.70	24.34	23.37
8×24 PULPv1	**37.95**	**33.07**	**29.06**	25.91	**24.59**	23.62
8×24 PULPv2	37.45	32.61	28.76	25.78	24.55	23.68
8×16 BOLPv11	37.84	33.02	29.04	**26.00**	24.55	23.49
8×16 BOLPv12	37.64	32.74	28.80	25.94	24.38	**23.80**

Fig. 11. Enlarged portions of the Barbara image compressed at 1:64 using various linear phase filter banks: 8×8 DCT (top-left), 8×16 LOT (top-middle), 8×24 1-regular PULP filter bank (top-right), 8×24 2-regular PULP filter bank (bottom-left), 8×16 (1,1)-regular BOLP filter bank and 8×16 (1,2)-regular BOLP filter bank.